12th International Congress on the Deterioration and Conservation of Stone
Columbia University, New York, 2012

PERFORMANCE OF NANOCOMPOSITES FOR CONSERVATION OF ARTISTIC STONES

Franca Persia,[1] Luisa Caneve,[2] Francesco Colao,[2] Rosaria D'Amato,[2]
Cristina Giancristofaro,[1] Giulia Ricci,[1] Luciano Pilloni[1] and Antonio Rinaldi[1]

[1] *ENEA-UTTMAT, S. Maria di Galeria (Rome), Italy*
[2]*ENEA-UTAPRAD Frascati (Rome), Italy*

Abstract

Properties of consolidant and protective materials modified with nanoparticles were analyzed following their application onto marble and travertine samples. To this purpose different solutions of an acrylic resin and a silicon-based polymer with dispersed silica and titania nanoparticles were prepared. Artificial aging processes, both in a climatic chamber and a solar box, were carried out to simulate real degradation processes in terms of photo-thermal effects and mechanical damage. The relative durability of the two different consolidants as modified by nanoparticles was evaluated by means of diverse diagnostic techniques, namely: scanning electron microscopy (SEM), laser induced fluorescence (LIF), ultrasonic velocity, colorimetry, total immersion water absorption and contact angle. The results indicate that nanoparticles enhance the effectiveness of consolidant and protective materials by inducing substantial changes of surface morphology of the coating layer and by countering physical damage during artificial weathering, especially in alkylsiloxane products.

Keywords: stone conservation, marble, travertine, nanocomposites, hydrophobic coatings, artificial weathering

1. Introduction

In recent years, nanocomposites have been frequently applied to restoration and conservation of artworks (Mosquera 2008; Manoudis 2009; Kima 2009). In fact, inorganic oxide nanoparticles, such as silica and titania, improve the performance of materials used in conservation field.

Consolidant, protective and hydrophobic polymeric materials have been used in conservation science for several decades (Torraca 1986; Tabasso 2006; Accardo 1981). Their protective properties were studied with regard to different aspects, such as different types of stones, natural and artificial environmental factors (e.g. water, solar light, chemical and biological pollutants, etc.), and degradation mechanisms (Favaro 2006; Kaczmarek 1996; Melo 1999).

Water, in any physical state, is a major degradation factor, due to its capability to transport chemical and biological substances in and out of the material, as well as to cause cracking in freeze-thaw and wet-dry cycles. The effect of water depends on the pore structure, which is responsible of these phenomena in first place (Amoroso 1983; Lazzarini 1986; Rodrìguez-Gordillo 2006).

For these reasons, consolidant properties and water repellency are often the most important requirement of a conservation product. Recently, the effectiveness of polymeric conservation products was improved by means of nanocomposites (Manoudis

2007, 2008; Shi 2008; Miliani 2007), which can be synthesized by different methods depending on the specific aim (Manoudis 2008).

In the present work, SiO_2 and TiO_2 nanoparticles, with size of about 15 nm and produced by CO_2 laser pyrolysis, were added as filler to acrylic and siloxane polymeric dispersions. Silica and titania were chosen for their physical properties, such as the improved water repellency (Shang 2005) following the increased roughness. As confirmed by scanning electronic microscopy (SEM), the roughness achieved from adding nanocomposites resembled the well-known surface properties of the lotus leaf, which confers self-cleaning and superhydrophobic properties (Manoudis 2009).

The preservation properties of the nanocomposites in the research were tested by the application on two different lithotypes, very common in outdoor cultural heritage: white marble (statuary and veined Carrara) and travertine. Samples of treated stone were submitted to artificial aging processes, both in climatic chamber and in solar box, to assess and compare the performance of nanocomposites.

Among the many techniques capable for testing the consolidant and the hydrophobic performance of the individual nanocomposites, non-invasive diagnostic techniques were chosen and deployed before and after the artificial aging processes, i.e. (i) SEM to check surface morphology, (ii) ultrasonic velocity to evaluate the effectiveness of the applied products in improving substrate cohesion, (iii) laser induced fluorescence (LIF) to recognize and discriminate different types of nanocomposites, (iv) colorimetric measurements to evaluate colour alteration, (v) contact angle to measure surface wettability, and (vi) water absorption through total immersion to calculate the relative imbibing capacity.

2. Experimental

2.1 Materials

Laboratory experiments were carried out on quarried travertine samples from Tivoli (Rome, IT, 5x5x4 cm) and on square blocks of three different types of marble: (i) Carrara with grey veins, (ii) white statuary Carrara (5x5x2 cm), and (iii) 8 pieces of historical marble of irregular size from the deposit of the National Roman Museum in Rome. Historical marbles were identified as Carrara, Proconnesio and Pentelic (Bosco 2009).

Before applying the conservation products, the white Carrara marble samples were aged naturally through open air exposure (inclined at 45° to the horizon, facing south) for 14 months. Carrara grey samples were aged through artificial weathering in climatic chamber by 10 freeze-thaw cycles (between 10h at -18°C to 10 h at 30°C). Prior to treatment, all the samples were washed with deionized water.

The nanocomposites were obtained by using two different commercial products as binders and two different nanoparticles as fillers with concentrations NP/polymer of 0.2, 1 and 2 (% w/vol). The two binders are commonly used for conservation of stone monument: 1. Paraloid B72, an acrylic resin (methylacrylate/ethylmethacrylate copolymer MA/EMA 30/70 w/w%) sold by SINOPIA, and, 2. Rhodorsil RC80, a polyethylsiloxane produced by Rhodia Silicones, Italy. The SiO_2 and TiO_2 nanoparticles were synthesised by CO_2 laser pyrolysis of two liquid precursors, $Si(OEt)_4$ and $Ti(i\text{-}OPr)_4$, respectively, with sizes around 15 nm and low polydispersity. The nanoparticles were used alone and together, with various mixing ratios. For the formulations based on

Paraloid B72, the calculated amount of nanoparticles were firstly dispersed in nitro solvent (GOLD 18, ITALCHIMICA LAZIO, IT) in different concentrations by using ultrasonic tip (Branson Sonifier 450) in order to obtain homogeneous dispersions. Then, 300 mg of Paraloid B72 were added to the different solution. For the formulations based on polyethylsiloxane the nanoparticles were directly dispersed in the commercial solution Rhodorsil RC80 and treated with ultrasonic tip for 20 minutes.

The solutions were applied on the stones by brushing until refusal to simulate the treatment in real situations as performed by a restorer. The treatment was repeated after 4 hours (Ferreira Pinto 2008).

2.1 Aging

Artificial aging by sunlight and freeze-thaw cycles was performed to evaluate the durability of the treated samples. A climatic chamber (SOLARBOX 1550 E) equipped with a xenon arc light source, 1500 W with spectral range from 280 to 800 nm was used. Following the standard UNI 10925-2001, samples underwent constant irradiation of 1000 W/m^2 for 556 hours. The irradiation time was sufficient to insure 2000 MJ/m^2, the specific irradiation conditions required by the standard. Twenty samples (from white and grey Carrara and 8 historical specimens) were treated.

The freeze-thaw resistance was carried out in an Angelantoni climatic chamber as per UNI EN 539 - 2. Accordingly, samples were first immersed in water for 7 days until complete imbibition of water. Then, 50 freeze-thaw cycles were carried out by slowly decreasing the temperature (over 15 minutes) down to -16±3°C, followed by a gradual increase (over 15 minutes) up to 17 °C, with hold times of 15 minutes between the ramps.

2.2 Evaluation tests

Scanning electron micrographs were collected to investigate the nanoparticle composite film morphologies and to evaluate the influence of nanoparticles on the integrity of surface coatings after the aging processes. The microstructural investigations were performed with a FEG-SEM LEO 1530 (Zeiss, Obercoken-Germany) equipped with In-lens secondary electron detector, conventional secondary electron detector and scintillation detector for backscattered electrons (Centaurus). The observations were carried out at low voltage in order to reduce charging effects due to the insulating nature of the applied polymeric films. The low voltage technique allowed observing the true surface morphology of insulating materials eliminating the artifact created by the usual metallisation.

The wettability properties of the nanocomposite coatings were assessed by static water contact angle measurements to evaluate the local water repellence of the surface. The measurements were carried out through a custom apparatus made in-house in compliance with standard UNI EN 15802 – 2010. The specimens were placed on a sample holder (free to translate in XYZ axes) and a 5 µl water drop was deposited onto the stone surface through a graduated micro-pipette. A stereo microscope Leica Wild M3Z connected to a digital camera (Moticam 2000) was used to acquire the drop image. The contact angle analysis was performed by the Low-Bond Axisymmetric Drop Shape Analysis (LBADSA) Plugin for ImageJ software, which is based on the fitting of the Young-Laplace equation to the image data (Stalder 2010).

Measurements of water absorption by total immersion were carried out to verify the water absorption capability. The used method is the gravimetric one with which the absorption curve and the relative Imbibing Capacity (I.C.) was measured for each sample. The results are presented according to UNI 10921 in terms of protection ratio percentages, P.R.%, which is defined as the percentage variation between the imbibing capacity of untreated and coated stone.

Ultrasonic velocity measurements (US) were carried out with a portable instrument, a Krautkramer USM 23 with low frequency using a probe of 50 KHz through transmission method and no sample preparation was necessary. Ultrasonic wave velocity was measured in all specimens in the three directions X, Y, and Z. For each direction, four values were recorded and the average was calculated. A thin layer of water was used as acoustic coupling medium between the stone and the transducer.

LIF measurements were performed with an apparatus realized at the ENEA laboratory. The radiation source is a Thomson DIVA diode pulsed Nd:YAG laser able to produce laser pulses both at 266 and 355 nm at a repetition rate of 20 Hz with a time duration of 8 ns. A laser fluence of 0.9 mJ/cm^2 was selected in this case. The detected spectral range was 200-800 nm and the spectrometer entrance was protected from the intense backscattered radiation by means of an appropriate filter. Since no optical elements were used to collimate the laser beam, the overall spatial resolution is a function of the operation distance and in the present case it was possible to infer a resolution of approximately 1 to 2 mm from the spot size on the target. The digitized spectrum was transferred to a portable computer where a LabView program allowed the user to set experimental parameters, to control data acquisition, and to perform a preliminary data analysis.

Colorimetric measurements were executed to calculate colour changes induced by photochemical and photothermal degradation of nanocomposite. Colour values, reported in the CIEL*a*b* space, were obtained using a Minolta CM-525i Spectophotometer, using a D65 illuminant. These results allowed calculating the total color difference ΔE, relative to the same area of the sample before and after coatings application.

US, LIF, SEM, contact angle, water absorption and colorimetric measurements were performed before and after each treatment and after the accelerated weathering tests.

3. Results and discussion

3.1 Results and discussion before aging

SEM images reveal that the surface morphology of the treated stone primarily depends on the nanoparticle concentration. Figure 1 shows the surface changes in Rhodorsil RC80 deposited films as a function of the silica nanoparticle concentration. The nanoparticles are not homogeneously dispersed in the polymer film, but they lead to the formation of protruded aggregates with irregular shape.

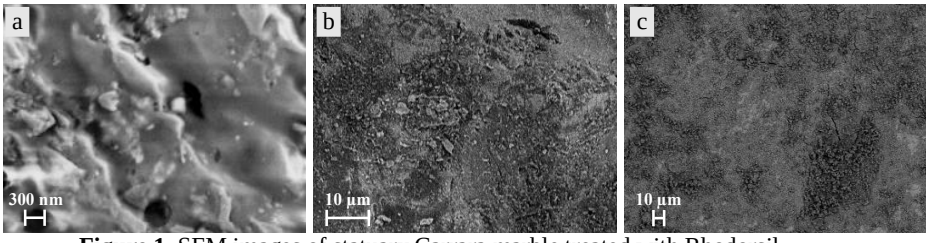

Figure 1. SEM images of statuary Carrara marble treated with Rhodorsil RC80 and 0.2% (a), 1% (b), 2% (c) w/v silica nanoparticles.

Few distinct aggregates separated by wide smooth areas of continuous polymer film can be observed on samples covered with polymeric low particle concentration films (0.2% w/v, Figure 1a). The increase in nanoparticles concentration (Figure 1b and c) enhanced the surface roughness of the stone because the protruded aggregates formed by the treatment are significantly higher. TiO_2/SiO_2 nanoparticles composite films show a different surface morphology due to the different interaction between silica/titania nanoparticles and siloxane matrix. Nano-mixtures containing a reduced concentration of titania nanoparticles are able to form homogeneous coatings, with aggregates embedded inside a continuous protective film, as shown in Figure 2a and c. On the contrary, the RC80 - TiO_2 (1% w/v) - SiO_2 (0.1% w/v) application increases the inhomogeneity of the film, producing big aggregates followed by nanoparticles-free smooth regions. In fact, Figure 2b suggests that the randomly distribution of titania aggregates can create areas of continuous visibly cracked polymer film.

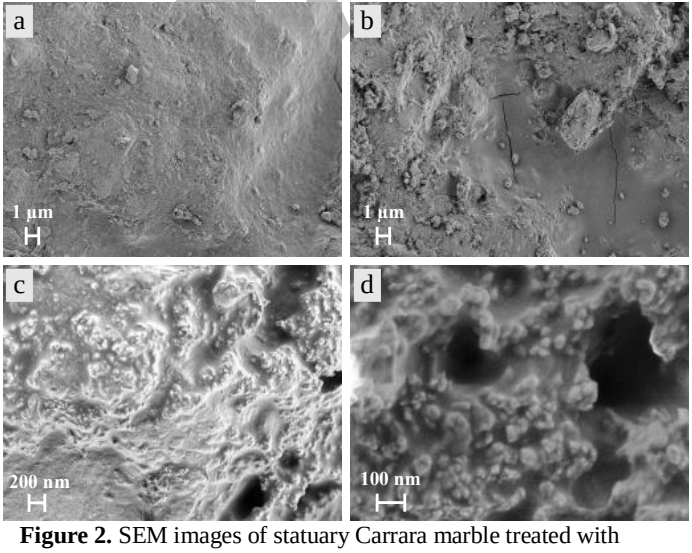

Figure 2. SEM images of statuary Carrara marble treated with (a) RC80 - SiO_2 (1%) - TiO_2 (0.1%), (b) RC80 - SiO_2 (0.1%) – TiO_2 (1%), (c,d) RC80 - SiO_2 (0.2%) - TiO_2 (0.2%).

SEM images of Paraloid B72+nanoparticles films were similar to the Rhodorsil ones. The size and the surface density of the aggregates were constantly proportional to

nanoparticle concentration.

The higher magnification SEM image (Figure 2d) reveals that the nanoparticle aggregate morphology induces a micro- and nano-scale roughness at the surface of the films. This effect is more evident for the acrylic composite. In fact, the acrylic film creates a smooth coating that suppresses the stone roughness. On the contrary, the pure siloxane forms a continuous film, which follows the underlying substrate with more fidelity, conserving the stone original roughness.

Figure 3 (left) shows the increase of static water contact angle (θs) as a function of SiO_2 particle concentration for Rhodorsil and Paraloid B72 composite films. In the case of Rhodorsil treatments we obtain a significant contact angle enhancement from about 110° (no particles) to almost 160° (2% w/v particles). Paraloid B72-SiO_2 values increase from around 80° (no particles) to 135° (2% w/v particles). The addition of titania nanoparticles gives comparable results for both kinds of investigated polymer coatings.

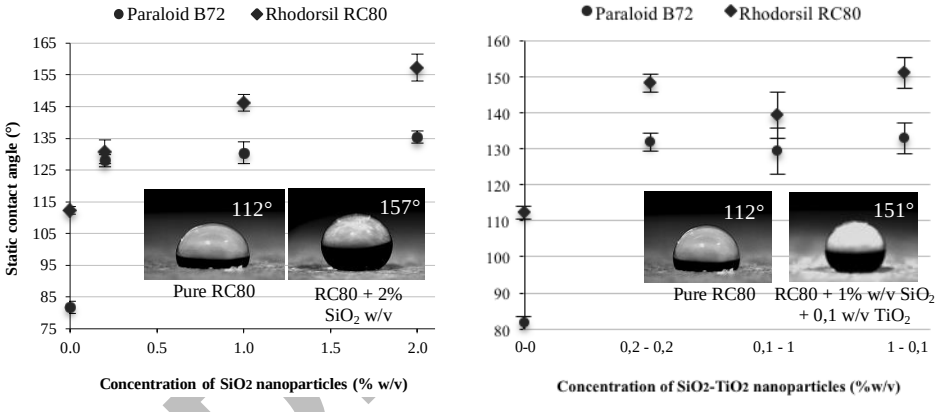

Figure 3. Static contact angle vs. concentration of silica nanoparticles (left) and SiO_2-TiO_2 nanomixtures (right).

The graph in Figure 3 (right) shows the water contact angles regarding silica and titania nanoparticle mixtures where an increasing up to 151° for siloxane films and up to 133° for acrylic nanocomposites is visible.

These data suggest that nanoparticles induce a significant enhancement in hydrophobicity and impart highly water repellent properties to the protective films. In particular Paraloid B72 protective layers change their character from hydrophilic (θs<90°) to hydrophobic (θs>90°) surface (Shang 2005).

SEM and contact angle analyses provided a useful insight in terms of good hydrophobicity and acceptable homogeneous surface morphology so that it was possible to select the optimal nanoparticle concentration for each kind of nanocomposite (silica-RC80, titania-RC80, silica and titania mixture-RC80) for subsequent analysis.

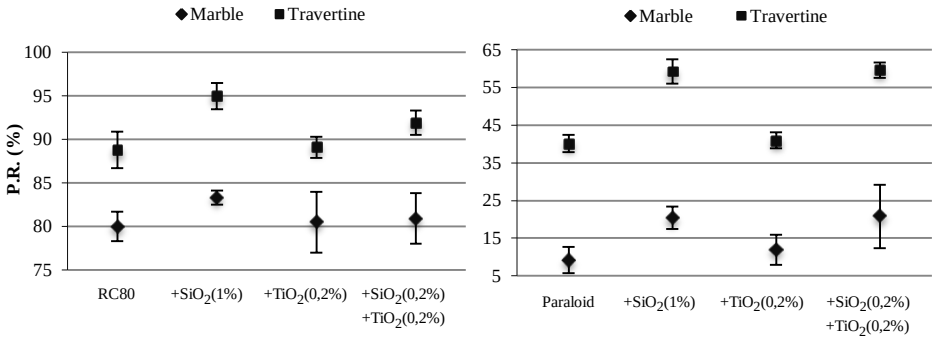

Figure 4. Protection Ratio (%) for marble and travertine substrates treated with Rhodorsil RC80 (left) and Paraloid B72 nanocomposites (right).

Figure 4 reports the Protection Ratios obtained for marble and travertine samples treated with siloxane and Paraloid B72 dispersions. The application of pure Rhodorsil RC80 decreases substantially the amount of water absorbed by the stone block. In fact the relative PR% are above 80% and 88% for marble and travertine substrates, respectively. The application of nanoparticle-modified dispersions increases the protective efficiency of the coatings. In fact the best performance is recorded for silica nanocomposites where P.R.% reaches up to 95% (on travertine specimen). The stones treated with titania composites rendered values similar to the pure siloxane. Silica-titania mixture shows an intermediate behavior.

The water absorption data obtained for Paraloid B72 dispersions once again demonstrate the enhanced efficiency of nanoparticles for marble and travertine protection. Indeed specimens treated with pure Paraloid B72 achieve P.R.% of order of 10% for marble and 40% for travertine, while by the application of nanocomposites containing silica or silica-titania mixture nanoparticles the P.R.% values raise to around 20% and 60% for marble and travertine respectively.

Measurements of ultrasonic velocity provided information concerning the effect of treatments on the mechanical properties of the stone. After the consolidation treatments, all the samples show an increase of ultrasonic velocity with respect to the untreated specimens due to the improvement of structural cohesion and mechanical resistance of marble and travertine substrates.

The US results show for both marbles and travertines a significant variation with siloxane treatment, while Paraloid B72 increase reached only 5% (Figure 5). This effect can be attributed to the low penetration capacity of the acrylic resin, partially ascribed to its high macromolecular dimensions that reduced the consolidation effect of the treatment by remaining in

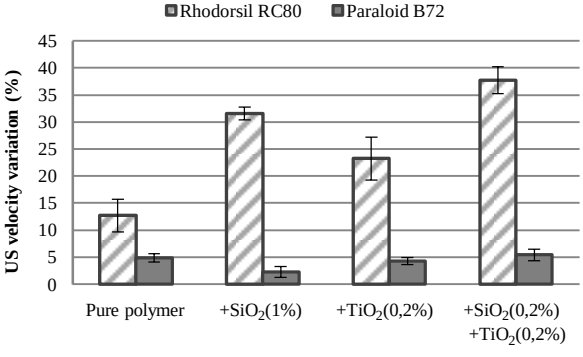

Figure 5. Ultrasonic velocity variation (%) in marble samples after the consolidation treatment

the more external zone of the stone samples. Higher enhancement of cohesion from the presence of silica nanoparticles results for Rhodorsil RC80 dispersions: the best performance were recorded with the addition of the silica and titania mixture at the same nanoparticle concentration of 0,2% w/v (about an ultrasonic velocity variation over 25% with respect to the pure siloxane application).

The fluorescence measurements have been carried out on the polymers and on the dispersions separately, at first. LIF spectra of both of RC80 and Paraloid B72 at the excitation wavelength of 266 nm present typical emission bands at 330 nm and 510 nm. The presence of nanoparticles determines a variation of the bands intensity (Figure 6). In particular, the band intensity at 510 nm increases in the presence of SiO_2, while the band disappears in the presence of TiO_2. Also in the mixed nanocomposites, the intensity increases when SiO_2 concentration increases, whereas it decreases if the TiO_2 quantity increases, confirming the photoluminescence properties of the nanosilica composite, as reported in the literature (Borsella 1997).

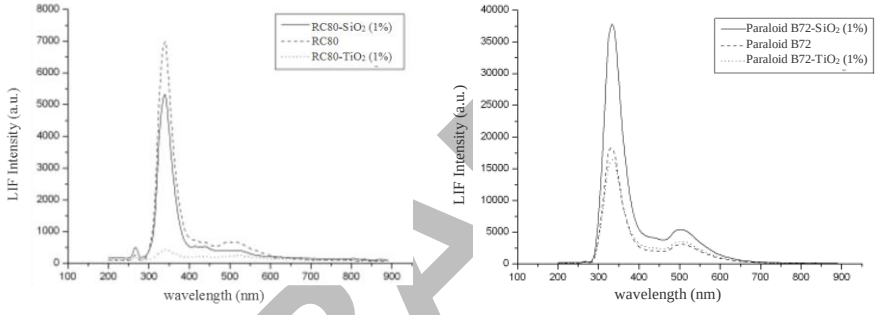

Figure 6. LIF spectra of silica and titania nanocomposites (1% w/v nanoparticle concentration) compared to pure RC80 and Paraloid B72 spectra

By the comparison of the lithotypes fluorescence spectra with those obtained from the treated stones it can be observed that the emission bands of the substrates at 355 nm overlap the fluorescence bands of RC80 and Paraloid B72, not permitting to discriminate the nanocomposites from the substrates themselves. The excitation wavelength of 266 nm, on the contrary, allows to observe some differences.

For Rhodorsil RC80 and Paraloid B72 treatments, the addition of SiO_2 nanoparticles causes an increase for 345 nm - 366 nm and 505 nm bands with respect to the pure polymer matrix. The presence of TiO_2 decreases the signal intensity, in different bands ratios related to the acrylic and siloxane matrix, differently. In the case of travertine the missing fluorescence of the substrate in the wavelength range of the polymers emissions permits to exactly identify a characteristic band of polymers at 340 nm. Also in this case, SiO_2 nanocomposites increase the fluorescence efficiency, while TiO_2 decreases the signal.

Colorimetric measurements show in RC80 films a maximum total color difference for marble surface treated with pure (no particles) polymer (ΔE=3.2; Figure 7). The addition of silica and titania nanoparticles prevents the brightness variation and reduces the global color difference ΔE. The travertine treated substrates undergoes a less important optical alteration due to the lower decrease of L* (ΔE=1.5). The nanoparticle filler is always able to reduce the total color difference ΔE.

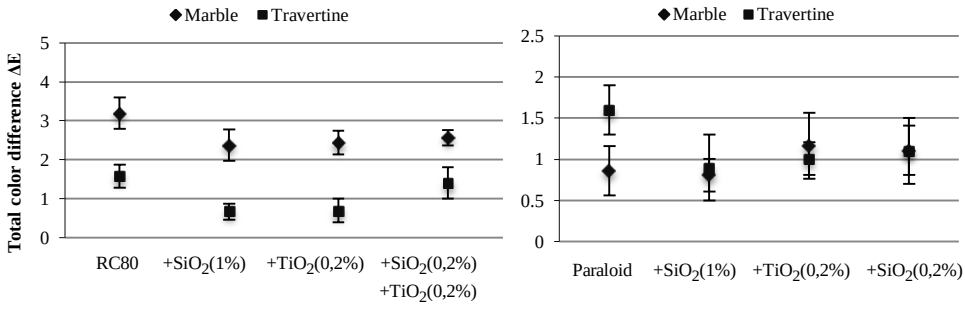

Figure 7. Total color difference ΔE for marble and travertine substrates treated with Rhodorsil RC80 (left) and Paraloid B72 nanocomposites (right)

The Paraloid B72 nanoparticle coatings determine on marble and travertine substrates similar slight color difference mainly caused by small changes in L* and b* (yellow–blue chromatic component). Pure Paraloid B72 application induces on travertine samples the most pronounced L* and b* variations. The polymer-particle composite films reduce this effect restoring the brightness of the stone.

The ΔE is <3 for all the nanocomposite specimens allowing to consider the color changes totally acceptable.

3.2 Results and discussion after aging

The photo-oxidative and mechanical aging tests reveal important different degradation processes clearly related to the selected exposure conditions and to the specific chemical and physical nanocomposite properties. The specimens exposure to the Solarbox irradiation shows for the siloxane treatments a good surface resistance due to the minimal morphological variation observed in SEM images and to the permanently characteristic luminescence bands in the acquired LIF spectra. On the contrary, Paraloid B72 irradiated films show in SEM images relevant surface alteration: an increase of pores, similar to the pitting phenomena corrosion, and loss of the polymeric material, individuated also in presence of nanofiller (Figure 9). The LIF spectra confirm this weathering: the luminescence band at 330 nm, characteristic of the acrylic polymer, disappears (Figure 8). This strong signal decrease can be due to reactions of photochemical degradation. In fact, changes in the molecular structure, as alterations in the unsaturated functional groups (carboxylic and carbonyl) responsible of the fluorescence processes, could be occurred.

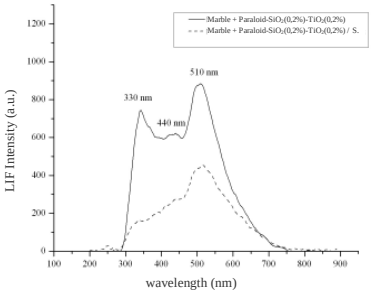

Figure 8. LIF spectra of a marble sample treated with a Paraloid B72 nanocomposite before and after Solarbox (S.) aging.

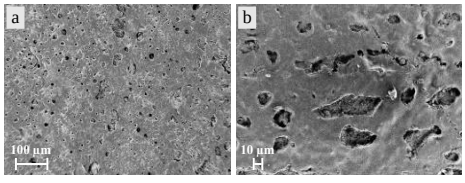

Figure 9. SEM images of grey Carrara marble treated with Paraloid B72 (a) and Paraloid B72/SiO_2 (b) after Solarbox aging

Water absorption properties and ultrasonic velocity variation after aging processes are in agreement with SEM and LIF results, confirming a correspondence between the surface properties and the consolidant effect. The siloxane dispersion shows the highest water absorption resistance (P.R. % equal to 83%) for nanosilica composites. The same result has been registered for acrylic treatment, showing a P.R. equal to 17%. The major total loss of protection effectiveness, well visible in RC80 compounds, is linked to the minor protection capability of the degraded acrylic film. The hydrophobicity of the stone specimens, measured through contact angle, undergoes a visible reduction in all nanocomposite surfaces (Table 1). At the end of the degradation process nanosilica composites nevertheless retain the greatest contact angle.

Treatment	CA (°)	D.S.	Aging	CA_i (°)	D.S.	ΔCA(°)	ΔCA (%)
RC80	112,4	1,2	S.	110,5	4,8	-1,9	-1,7
			F-T	112,1	4,2	-0,3	-0,3
RC80 - SiO_2 (1%)	146,2	2,6	S.	120,6	3,1	-25,6	-17,5
			F-T	129,5	3,0	-16,7	-11,4
RC80 - TiO_2 (0,2%)	131,5	3,0	S.	114,9	2,2	-16,6	-12,6
			F-T	126,1	4,0	-5,4	-4,1
RC80 - SiO_2 (0,2%) - TiO_2 (0,2%)	148,3	8,1	S.	114,7	1,7	-33,6	-22,7
			F-T	125,4	4,1	-22,9	-15,5
Paraloid B72	81,8	1,9	S.	71,2	2,2	-10,6	-13,0
			F-T	76,1	3,2	-5,7	-7,0
Paraloid B72 - SiO_2 (1%)	130,4	6,4	S.	115,1	3,1	-15,3	-11,7
			F-T	114,4	2,6	-16,0	-12,2
Paraloid B72 - TiO_2 (0,2%)	115,2	2,9	S.	105,2	1,4	-10,0	-8,7
			F-T	110,2	1,7	-5,0	-4,3
Paraloid B72 - SiO_2 (0,2%) - TiO_2 (0,2%)	131,8	2,6	S.	98,2	13,7	-33,6	-25,5
			F-T	110,1	2,5	-21,7	-16,5

Table 1. Static contact angle before (CA) and after (CA_i) Solarbox (S) and freeze-thaw (F-T) aging and relative standard deviation (D.S.). Static contact angle variation is also reported.

The physical-mechanical processes induced by freeze-thaw cycles allow to record a loss of conservation efficiency mainly detected by ultrasonic velocity and water

absorption data. The ultrasonic wave velocity shows a reduction of 50% for RC80 and 35% for Paraloid B72, without important variation related to the addition of nanoparticle filler. The loss of mechanical consistency responsible for these results brings a decrease of the protective capacity maintaining in any case the best performance of long-term durability and hydrophobicity (Table 1) for the nanosilica composites. LIF measurements after the aging processes on samples submitted to freeze-thaw cycles don't show differences on the spectra. No chemical variation of RC80 and Paraloid B72 is induced by this kind of treatment. Chromatic alteration measured in terms of ΔE is acceptable for all the specimens submitted to both kind of weathering aging, remaining <5.

4. Conclusions

Paraloid B72 and Rhodorsil RC80 modified with nanosilica and nanotitania have shown an appreciable enhancement of the conservation performances on both the tested specimens and the best behavior, in terms of protection capability and degradation durability, has been noted on the nanocomposite RC80/SiO_2 (1% w/v). A good resistance has been observed also in the samples treated with RC80/SiO_2 (0,2% w/v)/TiO_2 (0,2% w/v). Also for nano-modified Paraloid B72 the best performances have been observed with the addition of SiO_2 (1% w/v) nanoparticles and for the nano-oxides mixtures of SiO_2 (0,2% w/v)/TiO_2 (0,2% w/v).

The contact angle, measuring the wettability, has shown the nanoparticles capability to enhance the hydrophobicity in a conservation polymeric material inducing a better durability of the stone substrates treated by the different nanomixtures. This property becomes primarily important in case of artistic and monument stone expose to real outdoor conditions and extends the application of hydrophobic nanoparticle coatings to the field of cultural heritage conservation.

The colorimetric variations, measured before and after the accelerated aging processes, say that the optical surface alterations remain acceptable (ΔE value is always under 5).

SEM images and LIF spectra, allowing a morphological investigation and a molecular study on the treated stone surfaces, have shown that, after the aging, the greatest alteration has happened on the nano-modified acrylic polymer respect to those treated with nano-siloxane. The LIF technique presents the advantage to be a non-invasive and a remote application.

References

Accardo G., Cassano R., Rossi-Doria P., et al. 1981. 'Screening of products and methods for the consolidation of marble'. In *The conservation of stone, II: preprints of the contributions to the international symposium, Bologna, 27-30 October 1981*. Bologna: Centro per la conservazione delle sculture all'aperto.

Amoroso G.G., Fassina V. 1983. *Stone decay and conservation: atmospheric pollution, cleaning, consolidation and protection.* Amsterdam: Elsevier Science Publishers.

Borsella E., Botti S., Cremona M., et al. 1997. 'Photoluminescence from oxidised Si nanoparticles produced by CW CO_2 laser synthesis in a continuous-flow reactor'. *Journal of Alloys and Compounds*, **432**: L5–L9.

Bosco C. 2009. 'Studio dei trattamenti conservativi applicati su marmi tramite tecniche ottiche e spettroscopiche'. Thesis. University of Rome, La Sapienza.

Favaro M., Mendichi R., Ossola F., et al. 2006. 'Evaluation of polymers for conservation treatments of outdoor exposed stone monuments. Part I: Photo-oxidative weathering'. *Polymer Degradation and Stability*, **91**: 3083-3096.

Ferreira Pinto A.P., Delgado Rodrigues J. 2008. 'Stone consolidation: The role of treatment procedures'. *Journal of Cultural Heritage*, **9**: 38-53.

Kaczmarek H. 1996. 'Changes to polymer morphology caused by U.V. irradiation: 1.Surface damage'. *Polymer*, **37**(2): 189-194.

Kaczmarek H. 1996. 'Changes to polymer morphology caused by U.V. irradiation: 2.Surface destruction of polymer blends'. *Polymer*, **37**(4): 547-553.

Kima E.K., Won J., Dob J., et al. 2009. 'Effects of silica nanoparticle and GPTMS addition on TEOS-based stone consolidants'. *Journal of Cultural Heritage*, **10**: 214–221.

Lazzarini L., Tabasso M.L. 1986. *Il restauro della pietra*. Padova: Cedameditore.

Manoudis P., Papadopoulou S., Karapanagiotis I. et al. 2007. 'Polymer-Silica nanoparticles composite films as protective coatings for stone-based monuments'. *Journal of Physics*, Conference Series **61**: 1361–1365.

Manoudis P.N., Karapanagiotis I., Tsakalof A., et al. 2008a. 'Super-hydrophobic polymer/nanoparticle composites for the protection of marble monuments'. *9th International Conference on NDT of Art, Jerusalem Israel, 25-30 May 2008.*

Manoudis P.N., Karapanagiotis I., Tsakalof A., et al. 2008b. 'Superhydrophobic Composite Films Produced on VariousSubstrates'. *Langmuir*, **24**: 11225-11232.

Manoudis P.N., Karapanagiotis I., Tsakalof A., et al. 2009a. 'Fabrication of super-hydrophobic surfaces for enhanced stone protection'. *Surface & CoatingsTechnology*, **203**: 1322–1328.

Manoudis P.N., Karapanagiotis I., Tsakalof A., et al. 2009b. 'Superhydrophobic films for the protection of outdoor cultural heritage assets'. *Surface & Coatings Technology*, **203**: 1322–1328.

Melo M.J., Bracci S., Camaiti M., et al. 1999. 'Photodegradation of acrylic resins used in the conservation of stone'. *Polymer Degradation and Stability*, **66**: 23-30.

Miliani C., Velo-Simpson M.L., Scherer G.W. 2007. 'Particle-modified consolidants: A study on the effect of particles on sol-gel properties and consolidation effectiveness'. *Journal of Cultural Heritage*, **8**: 1-6.

Mosquera M.J., De los Santos D.M., Montes A., et al. 2008. 'New Nanomaterials for Consolidating Stone'. *Langmuir*, **24**: 2772-277.

Rodrìguez-Gordillo J., Sàez-Pérez M.P. 2006. 'Effects of thermal changes on Macael marble: Experimental study'. *Construction and Building Materials*, **20**: 355–365.

Shang H.M., Wang Y., Limmer S.J. et al. 2005. 'Optically transparent superhydrophobic silica-based films'. *Thin Solid Films*, **472**: 37-43.

Shi H., Liu F., Yang L., et al. 2008. 'Characterization of protective performance of epoxy reinforced with nanometer-sized TiO_2 and SiO_2'. *Progress in Organic Coatings*, **62**: 359–368.

StalderA.R., MelchiorT., Muller M., et al. 2010.'Low-Bond Axisymmetric Drop Shape Analysis for Surface Tensionand Contact Angle Measurements of Sessile Drops'.*Colloids Surf* A, **364**: 72–81.

Tabasso M.L., Simon S. 2006. 'Testing methods and criteria for the selection/evaluation of products for the conservation of porous building materials'. *Reviews in conservation*, **7**: 67-82.

Torraca G. 1986. 'Momenti nella storia della conservazione del marmo: Metodi e attitudini in varie epoche'. In *OPD restauro*: Quaderni dell'opificio dell pietra dure e laboratori di restauro di Firenze, numero speciale. Firenze: Opus Libri.